

BIO-GATS: A tool for automated GPCR template selection through a biophysical approach for homology modelling

Amara Jabeen¹, Ramya Vijayram², Shoba Ranganathan^{1,*}

¹ Department of Molecular Sciences, Macquarie University, Sydney, NSW 2109, Australia

² Department of Biotechnology, Bhupat and Jyoti Mehta School of Biosciences, Indian Institute of Technology Madras, Chennai 600036, Tamilnadu, India

* Corresponding author (shoba.ranganathan@mq.edu.au)

Supplementary Materials

Contents

Supp Table 1:	Detailed parameter listing and scoring of published target-template dataset.....	2
Supp Table 2:	RMSD calculation (TM only) between GPCR structures and models based on templates selected by Bio-GATS.....	5
Supp Figure 1:	The superimposed manual and automated models for class A orphans	6
Supp Figure 2:	The superimposed manual and automated models for class C orphans	7
Supp Table 3:	Template(s) selected by Bio-GATS and other servers for class A & C orphans ..	8
Supp Figure 3:	Helix-wise hydrophobicity correspondence between OR1A1 and 6HLP	9
Supp Figure 4:	Helix-wise hydrophobicity correspondence between OR1A1 and 1U19.....	10
Supp Figure 5:	Helix-wise hydrophobicity correspondence between OR1A1 and 6IIU	11
Supp Figure 6:	Helix-wise hydrophobicity correspondence between OR1A1 and 3ODU	12
Supp Figure 7:	Helical wheel plots from Bio-GATS for TM2 and TM3.....	13
Supp Figure 8:	Helical wheel plots from Bio-GATS for TM4 and TM5.....	14
Supp Figure 9:	Helical wheel plots from Bio-GATS for TM6 and TM7.....	15
Supp Note 1:	Bio-GATS result summary for OPSD_BOVIN-OR1A1_HUMAN	16
Supp Table 4:	Ligand profile comparison between OR1A1 and the selected templates	24
Supp Table 5:	The interactions of 1U19-based and 3ODU-based OR1A1 models with known ligands of OR1A1	25
Supp Figure 10:	The alignment generated by GPCR-I-TASSER	27
Supp Figure 11:	The alignment generated by GPCRM	27
Supp Figure 12:	The alignment generated by BIO-GATS between the query sequence (OR1A1) and the selected template, 1U19	28
Supp Figure 13:	The <i>Browse template</i> window with options	29
Supp Figure 14:	The <i>Available PDBs</i> window	30
Supp Figure 15:	The <i>SSD calculator</i> with customizable TM definitions.	31
Supp Figure 16:	The <i>Show alignment</i> window	32
Supp References	33

Supplementary Table 1: Detailed parameter listing and scoring of published target-template dataset as per our approach. SI is the sequence identity, S_h is the overall hydrophobicity correspondence score ranging from helix 1 to 7, S_b is the binding site residue similarity score and S_r is the resolution score. The target-template pairs with highest value of S_t (also shown in Table 1) are in bold

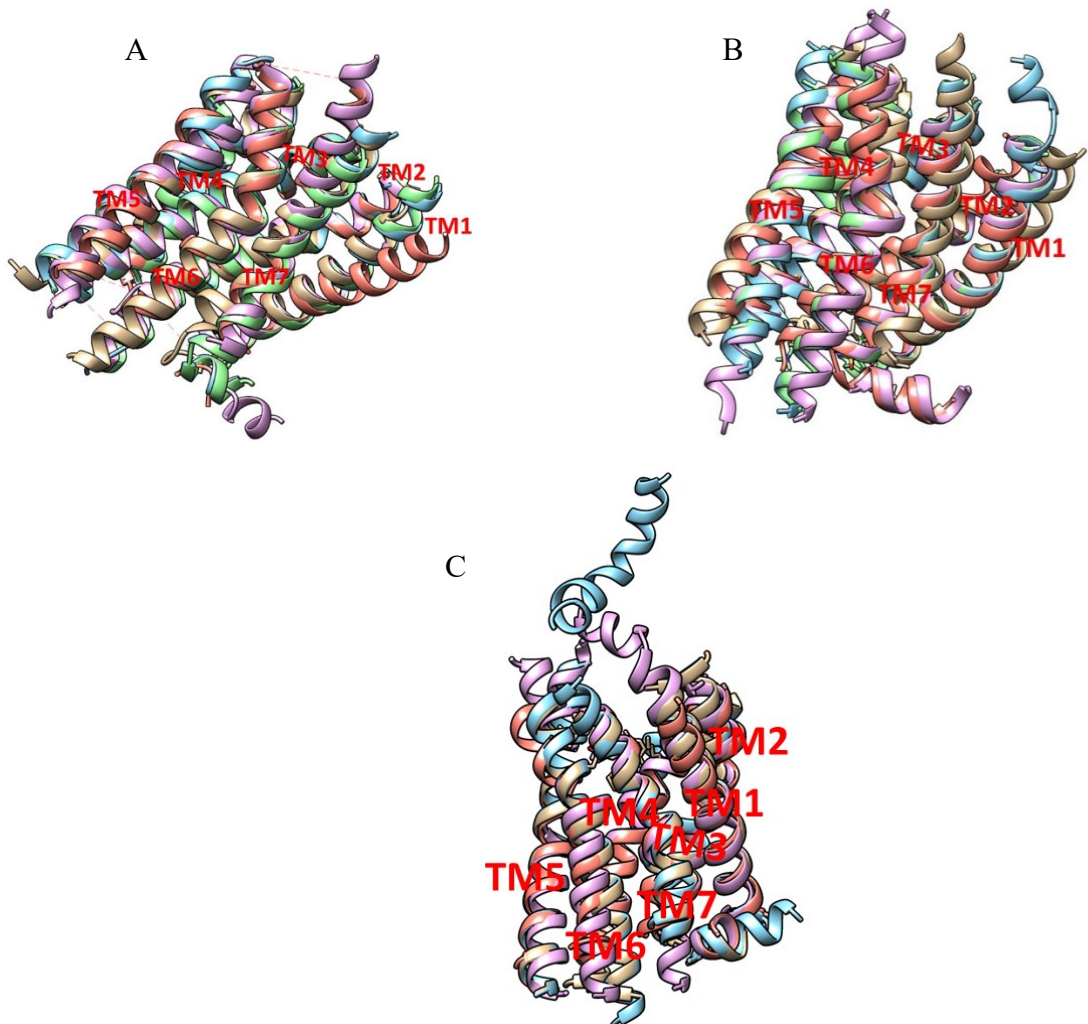
Target-template pairs	Res (Å)	Published ranking	SI (%)	SSD-TM1	SSD-TM2	SSD-TM3	SSD-TM4	SSD-TM5	SSD-TM6	SSD-TM7	S_h	S_b	S_r	S_t
PAR2_HUMAN- PAR1_HUMAN (PDBID: 3VW7) [1]	2.2	Good	41	0.047	0.008	0.052	0.048	0.018	0.054	0.008	12	39	1	52
PAR2_HUMAN - OPRX_HUMAN (PDBID: 4EA3)[1]	3.0	Good	28	0.016	0.023	0.041	0.092	0.049	0.01	0.034	13	18	0	31
PAR2_HUMAN - OPSD_BOVIN (PDBID: 1U19) [1]	2.2	Bad	22	0.02	0.012	0.038	0.05	0.06	0.093	0.012	11	-2	1	10
5HT7_HUMAN - OPRX_HUMAN (PDBID: 4EA3) [2]	3.0	Good	24	0.068	0.024	0.042	0.019	0.088	0.1	0.015	9	32	0	41
5HT7_HUMAN- PAR1_HUMAN (PDBID: 3VW7) [2]	2.2	Bad	27	0.042	0.031	0.078	0.045	0.074	0.027	0.045	12	17	1	30
PAR1_HUMAN - OPRK_HUMAN (PDBID: 4DJH) [3]	2.9	Good	27	0.032	0.024	0.044	0.042	0.038	0.058	0.017	13	29	0	42
PAR1_HUMAN- OPRX_HUMAN (PDBID: 5DHG) [3]	3.0	Good	27	0.041	0.018	0.056	0.037	0.068	0.067	0.03	11	29	0	40
PAR1_HUMAN – AA2AR_HUMAN (PDBID: 3EML) [3]	2.6	Bad	21	0.028	0.056	0.105	0.02	0.046	0.028	0.027	10	9	0	19
ADRB2_HUMAN - OPRK_HUMAN (PDBID: 4DJH) [3]	2.9	Good	24	0.063	0.073	0.012	0.041	0.117	0.116	0.073	5	26	0	31
ADRB2_HUMAN – AA2AR_HUMAN (PDBID: 3EML)[3]	2.6	Good	30	0.096	0.012	0.046	0.023	0.033	0.022	0.099	12	5	0	17
ADRB2_HUMAN- P2Y ₁₂ R_HUMAN (PDBID: 4NTJ) [3]	2.6	Bad	21	0.05	0.053	0.134	0.059	0.047	0.113	0.11	3	6	0	9

Target-template pairs	Res (Å)	Published ranking	SI (%)	SSD- TM1	SSD- TM2	SSD- TM3	SSD- TM4	SSD- TM5	SSD- TM6	SSD- TM7	S_h	S_b	S_r	S_t
P2Y ₁₂ R_HUMAN - PAR1_HUMAN (PDBID: 3VW7) [4]	2.2	Good	23	0.124	0.016	0.168	0.04	0.048	0.073	0.08	6	20	1	27
P2Y ₁₂ R_HUMAN- OPRK_HUMAN (PDBID: 4DJH) [3]	2.9	Bad	28	0.095	0.043	0.101	0.079	0.062	0.154	0.051	4	11	0	15
P2Y ₁₂ R_HUMAN - 5HT1B_HUMAN (PDBID: 4IAQ) [4]	2.8	Bad	24	0.05	0.034	0.14	0.066	0.04	0.116	0.12	2	8	0	10
P2Y ₁₂ R_HUMAN- ADRB2_HUMAN (PDBID: 2RH1) [3]	2.4	Bad	21	0.05	0.053	0.134	0.059	0.047	0.113	0.11	2	6	1	9
ACM2_HUMAN- DRD3_HUMAN (PDBID: 3PBL) [4]	2.9	Good	26	0.11	0.011	0.037	0.032	0.035	0.058	0.034	10	34	0	44
ACM2_HUMAN- OPRK_HUMAN (PDBID: 4DJH) [3]	2.9	Good	28	0.025	0.042	0.017	0.039	0.138	0.032	0.01	11	15	0	26
ACM2_HUMAN - P2Y ₁₂ R_HUMAN (PDBID: 4NTJ) [3]	2.6	Bad	23	0.059	0.05	0.122	0.102	0.037	0.101	0.077	2	1	0	3
FFAR1_HUMAN - AT1R_HUMAN (PDBID: 4YAY) [4]	2.9	Good	22	0.17	0.053	0.058	0.036	0.025	0.047	0.082	8	16	0	24
FFAR1_HUMAN - P2Y ₁₂ R_HUMAN (PDBID: 4PY0) [4]	3.1	Bad	27	0.106	0.033	0.175	0.069	0.044	0.072	0.032	6	16	0	22
5HT2AR_HUMAN-5HT2CR_HUMAN (PDBID: 6BQH) [5]	2.7	Good	55	0.02	0.008	0.01	0.005	0.008	0.012	0.053	13	58	0	71
5HT2AR_HUMAN - OPSD_BOVIN (PDBID: 1F88) [5]	2.8	Bad	20	0.062	0.025	0.041	0.055	0.039	0.014	0.03	12	8	0	20
5-HT2AR_HUMAN- AA2AR_HUMAN(PDBID: 4EIY) [5]	1.8	Bad	26	0.109	0.013	0.033	0.038	0.015	0.016	0.03	11	7	1	19
5HT2AR_HUMAN - CXCR4_HUMAN (PDBID: 3ODU) [5]	2.5	Bad	21	0.023	0.148	0.035	0.02	0.024	0.065	0.091	9	1	1	11

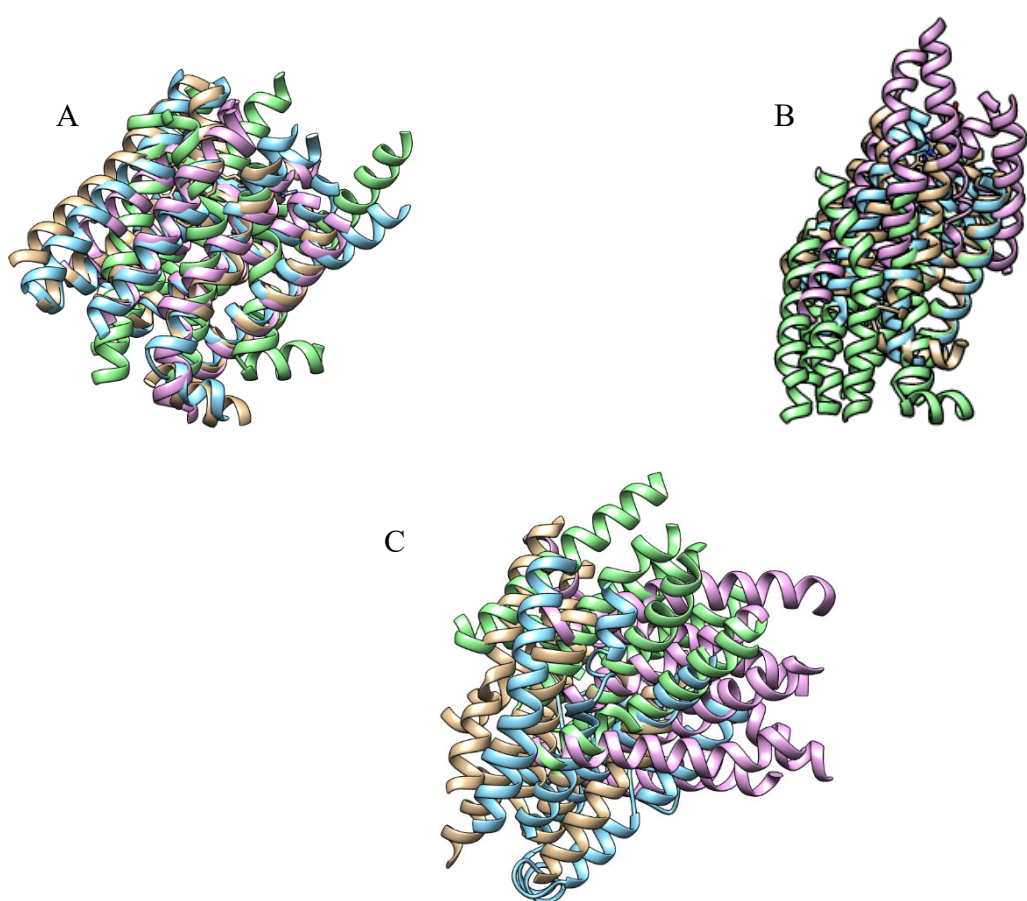
Target-template pairs	Res (Å)	Published ranking	SI (%)	SSD- TM1	SSD- TM2	SSD- TM3	SSD- TM4	SSD- TM5	SSD- TM6	SSD- TM7	S_h	S_b	S_r	S_t
5HT2AR_HUMAN -CNR1_HUMAN (PDBID: 5U09) [5]	2.6	Bad	27	0.061	0.03	0.085	0.044	0.033	0.032	0.049	12	-3	0	9
DRD2_HUMAN -CXCR4_HUMAN (PDBID: 3ODU) [5]	2.5	Good	29	0.063	0.19	0.034	0.039	0.09	0.036	0.037	9	16	1	26
DRD2_HUMAN - OPSD_BOVIN (PDBID: 1F88) [5]	2.8	Bad	22	0.102	0.028	0.058	0.096	0.118	0.054	0.021	5	6	0	11
DRD2_HUMAN -CNR1_HUMAN (PDBID: 5U09) [5]	2.6	Bad	25	0.132	0.053	0.044	0.069	0.142	0.022	0.036	6	-4	0	2

Supplementary Table 2: RMSD calculation (TM only) between GPCR structures and models based on templates selected by Bio-GATS. Human GPCRs are prefixed by h, mouse by m, yeast by y, turkey by t and bovine by b.

Class	Receptor	PDBID	State	Template selected by Bio-GATS with PDBID	RMSD (Å)
A	h5HT2A	6A94	inactive	tADRB1 (4BVN)	1.56
	h5HT2C	6BQH	inactive	hADRB2 (2RH1)	1.327
	hAA1AR	5UEN	inactive	hAA2AR (5IU4)	1.192
	hAA2AR	5IU4	inactive	tADRB1 (4BVN)	2.737
	hACM1	5CXV	inactive	hACM5 (6OL9)	2.50
	hACM2	5ZKC	inactive	hACM5 (6OL9)	1.203
	hADRB2	2RH1	inactive	tADRB1 (4BVN)	0.963
	hAGTR1	4YAY	inactive	hCCR7 (6QZH)	1.897
	hCCR2	6GPX	inactive	hCCR5 (5UIW)	1.243
	hCNR2	6KPC	inactive	hCCR7 (6QZH)	1.859
	hDRD2	6CM4	inactive	tADRB1 (4BVN)	1.714
	hDRD3	3PBL	inactive	tADRB1 (4BVN)	1.519
	hHRH1	3RZE	inactive	hACM5 (6OL9)	1.478
	hOPRD	4EJ4	inactive	hOX1R (6TOS)	1.836
	hOX2R	5WQC	inactive	hOX1R (6TOS)	0.844
	hS1PR1	3V2Y	inactive	hCCR7 (6QZH)	2.032
	hTA2R	6IIU	inactive	bOPSD (1U19)	2.342
	hPE2R3	6AK3	active	bOPSD (4X1H)	1.705
	hPTAFR	5ZKP	active	mOPRM1 (5C1M)	2.376
	hP2Y12	4PXZ	Intermediate	hEDNRB (6IGK)	2.254
B	hCRFR1	4K5Y	inactive	hGLR (5EE7)	1.753
	hGLP1R	5VEW	inactive	hGLR (5EE7)	1.349
	hGLR	5EE7	inactive	hPTH1R (6FJ3)	1.551
	hPTH1R	6FJ3	inactive	hGLR (5EE7)	1.614
	hCALRL	6UVA	active	hSCTR (6WZG)	1.539
	hCRFR2	6PB1	active	hCALRL (6UVA)	1.512
	hGHRHR	7CZ5	active	hSCTR (6WZG)	1.315
	hPACR	6P9Y	active	hSCTR (6WZG)	1.004
	hSCTR	6WZG	active	hCALRL (6UVA)	1.633
	hVIPR1	6VN7	active	hSCTR (6WZG)	1.133
C	hGABR1	6W2Y	inactive	hGABR2 (7C7S)	1.969
	hGABR2	7C7S	inactive	hGABR1 (6W2Y)	2.289
	hGRM1	4OR2	inactive	hGRM5 (6N52)	1.294
	hGRM5	6N52	inactive	hGRM1 (4OR2)	1.641
D	ySTE2	7AD3	active	hGLP1R(6X19)	2.416
F	hFZD4	6BD4	inactive	hPTH1R (6FJ3)	2.005
	hFZD5	6WW2	inactive	hPTH1R (6FJ3)	1.969
	hSMO	5V56	inactive	mSMO (6O3C)	1.986



Supplementary Figure 1: The superimposed manual and automated models for class A orphans:(A) GPR35, (B) P2RY8, and (C) P2RY10. The manual model generated on the basis of Bio-GATS template is shown in gold color, GPCRM model is shown in pink color, GPCR-SSFE model is shown in rust color, GPCR-modsim model is shown in green color, and GoMoDo model is shown in blue color. Template details are available in Supplementary Table 2.



Supplementary Figure 2: The superimposed manual and automated models for class C orphans: (A) GPC5C, (B) GPC5D, and (C) RAI3. The manual model generated on the basis of Bio-GATS template is shown in gold color, GPCR-MoDo model is shown in pink color, GPCR-Modsim model is shown in green color, and GoMoDo model is shown in blue color. Template details are available in Supplementary Table 2.

Supplementary Table 3: Template(s) selected by Bio-GATS and other servers for class A & C orphans with RMSD values calculated from structural alignment of models generated with the manual model. The human GPCRs are prefixed by h, mouse by m, and zebra fish by z.

Receptor	Selected template(s) with PDBID					RMSD (Å)
	Bio-GATS	GPCRM	GPCR-SSFE	GPCR-modsim	GoMoDo	
GPR35_Human (Class A-orphan)	5UIW (hCCR5)	6B73 (hOPRK), 4XNW (hP2RY1)	Many ¹	4EA3 (hOPRX)	4EA3 (hOPRX)	1.58
P2RY8_Human (Class A-orphan)	6QZH (hCCR7)	5NDD (hPAR2), 4DJH (hOPRK)	Many ²	3VW7 (hPAR1)	3VW7 (hPAR1)	1.71
P2Y10_Human (Class A-orphan)	4N6H (hOPRD)	5NDD (hPAR2), 4XNW (hP2RY1)	Many ³	None ⁵	4N6H (hOPRD)	1.50
GPC5C_Human (Class C-orphan)	3KS9 (hGRM2)	4OR2 (hGRM1), 5CGC (hGRM5)	None ⁴	2RH1 (hADRB2)	4IAR (h5HT1B)	2.98
GPC5D_Human (Class C-orphan)	5IU4 hAA2AR	4PY0 (hP2RY12) 6B73 (hOPRK)	None ⁴	4DJH (hOPRK)	4OR2 (hGRM1)	2.60
RAI3 (Class C-orphan)	5UIW (hCCR5)	5UIG, 4EIY (hAA2AR)	None ⁴	3UON (hACM2)	4OR2 (hGRM1)	3.62

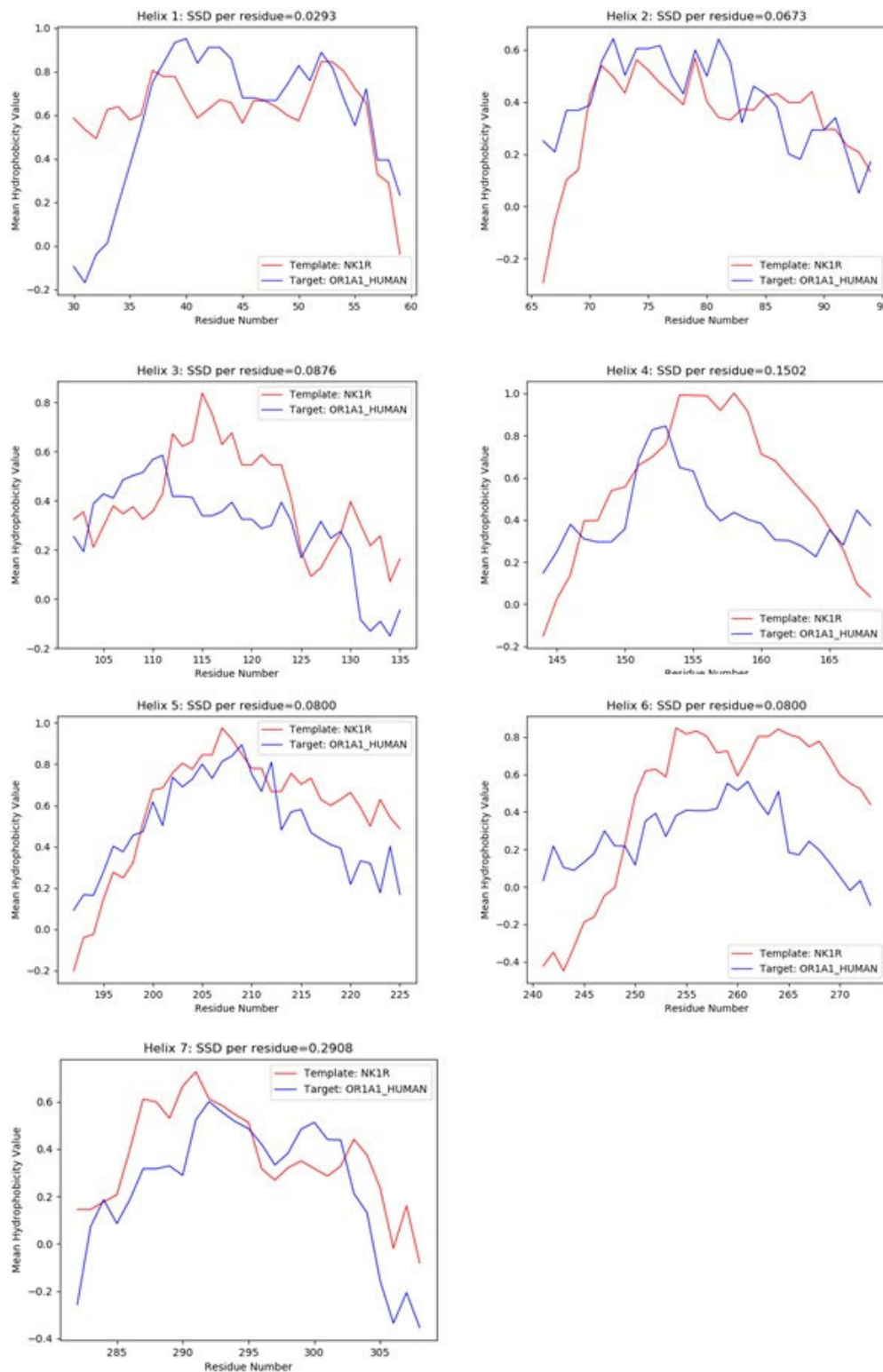
¹GPCR-SSFE templates: hOPRK1 (4DJH), hOPRL1 (4EA3), hCCR5 (4MBS), hCXCR4 (3ODU), mOPRD1 (4EJ4), zLPA6 (5XSZ)

²GPCR-SSFE templates: hPAR1 (3VW7), hDRD3 (3PBL), hOPRK1 (4DJH), hP2RY1_Human(4XNV), hCCR5 (4MBS), hPAR2 (5NDD)

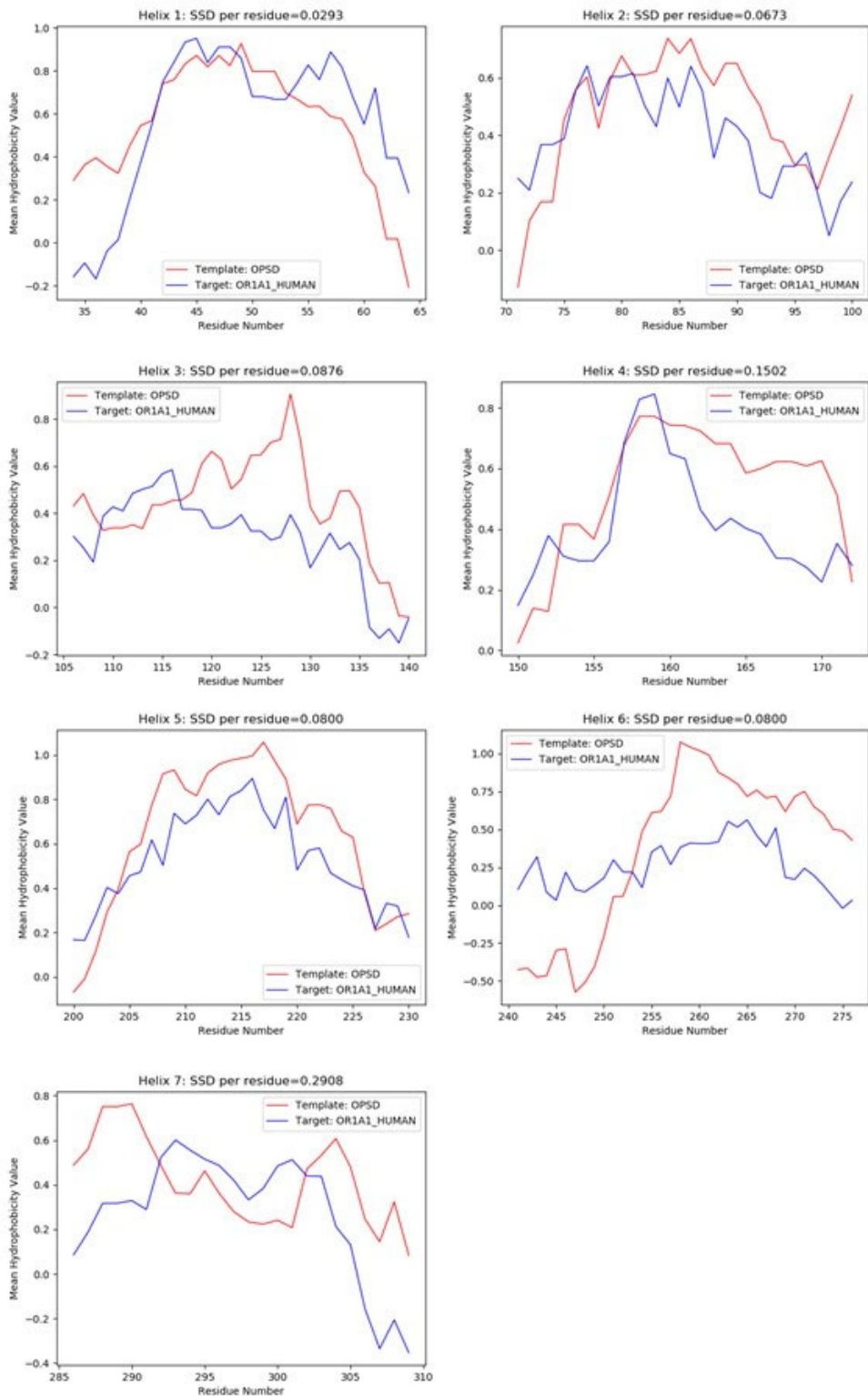
³GPCR-SSFE templates: hOPRK1 (4DJH), hPAR2 (5NDD), zLPA6 (5XSZ), hP2Y12 (4NTJ)

⁴GPCR-SSFE does not work on non-Class A GPCRs.

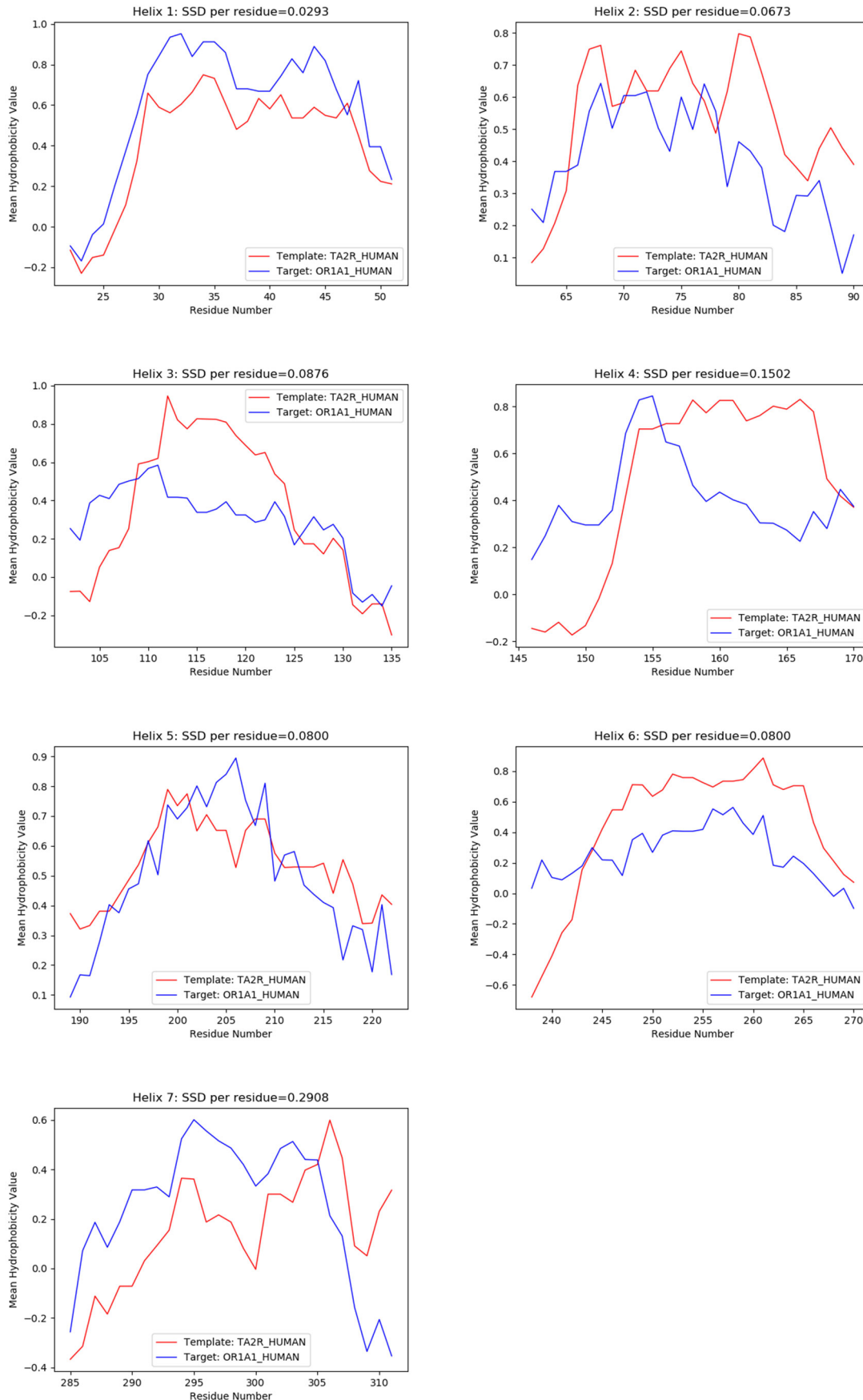
⁵GPCR-modsim does not work for hP2Y10.



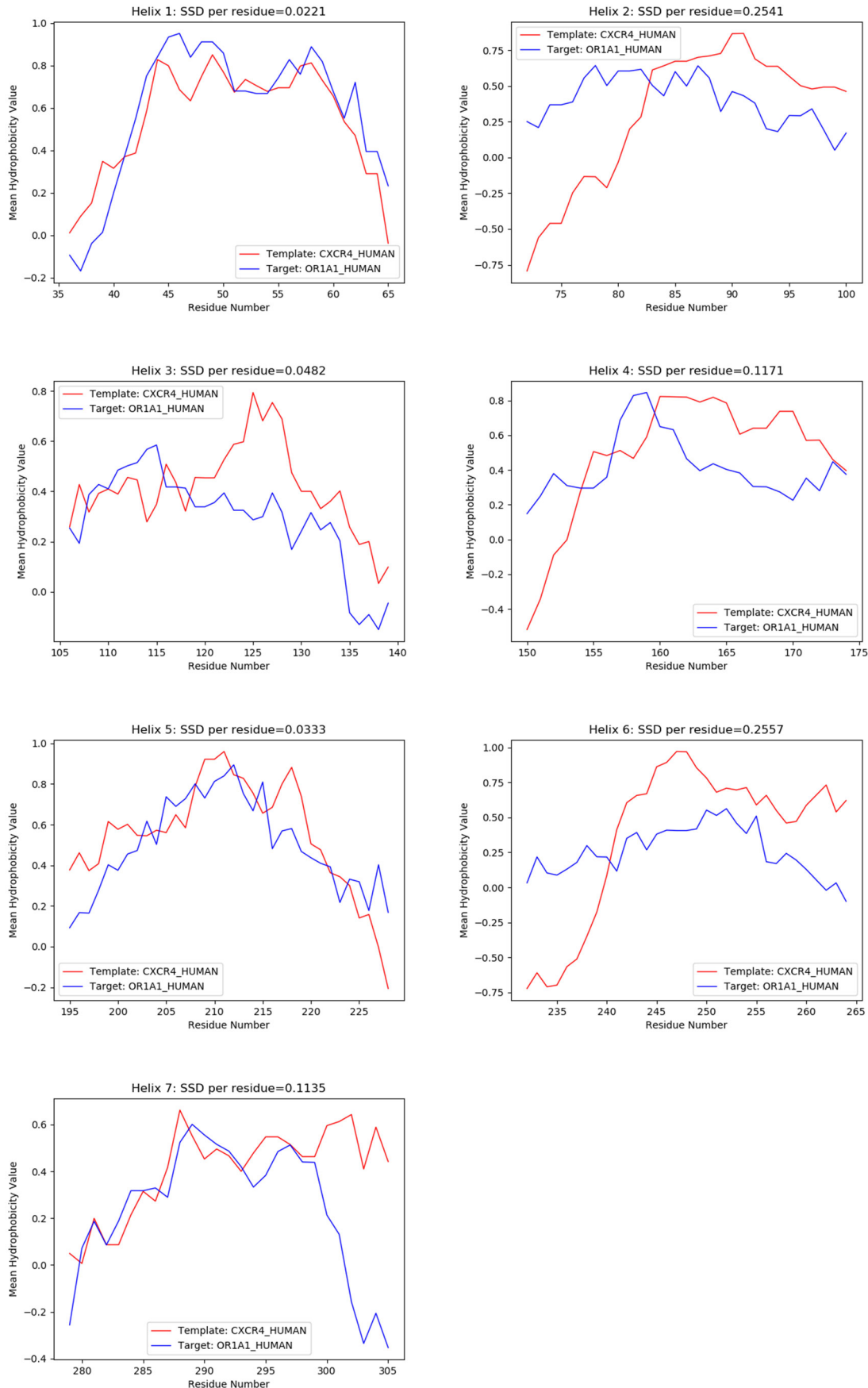
Supplementary Figure 3: Helix-wise hydrophobicity correspondence between OR1A1 and 6HLP (top template selected by Bio-GATS). Images are taken from Bio-GATS.



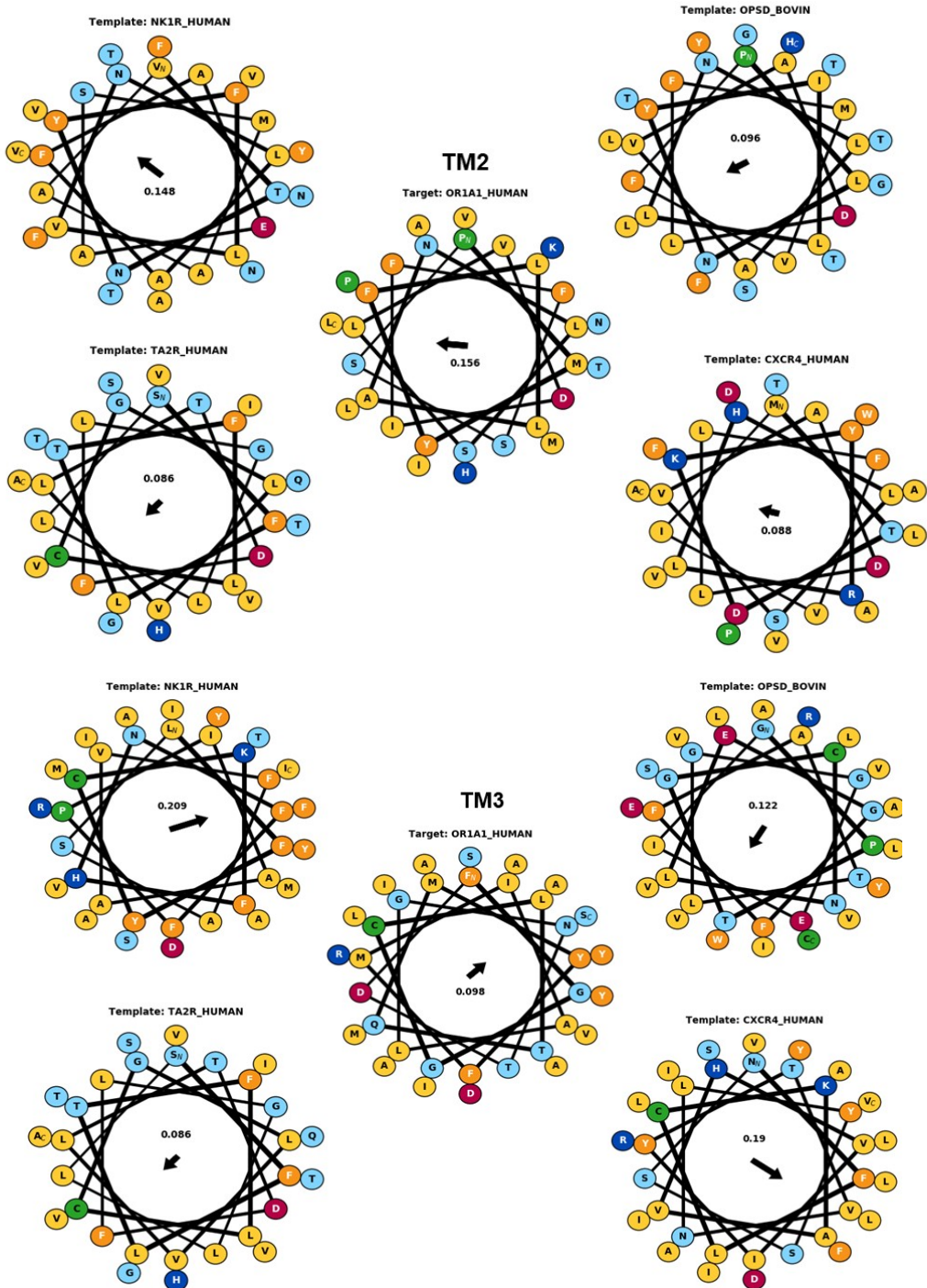
Supplementary Figure 4: Helix-wise hydrophobicity correspondence between OR1A1 and 1U19 (the 2nd best template by Bio-GATS).



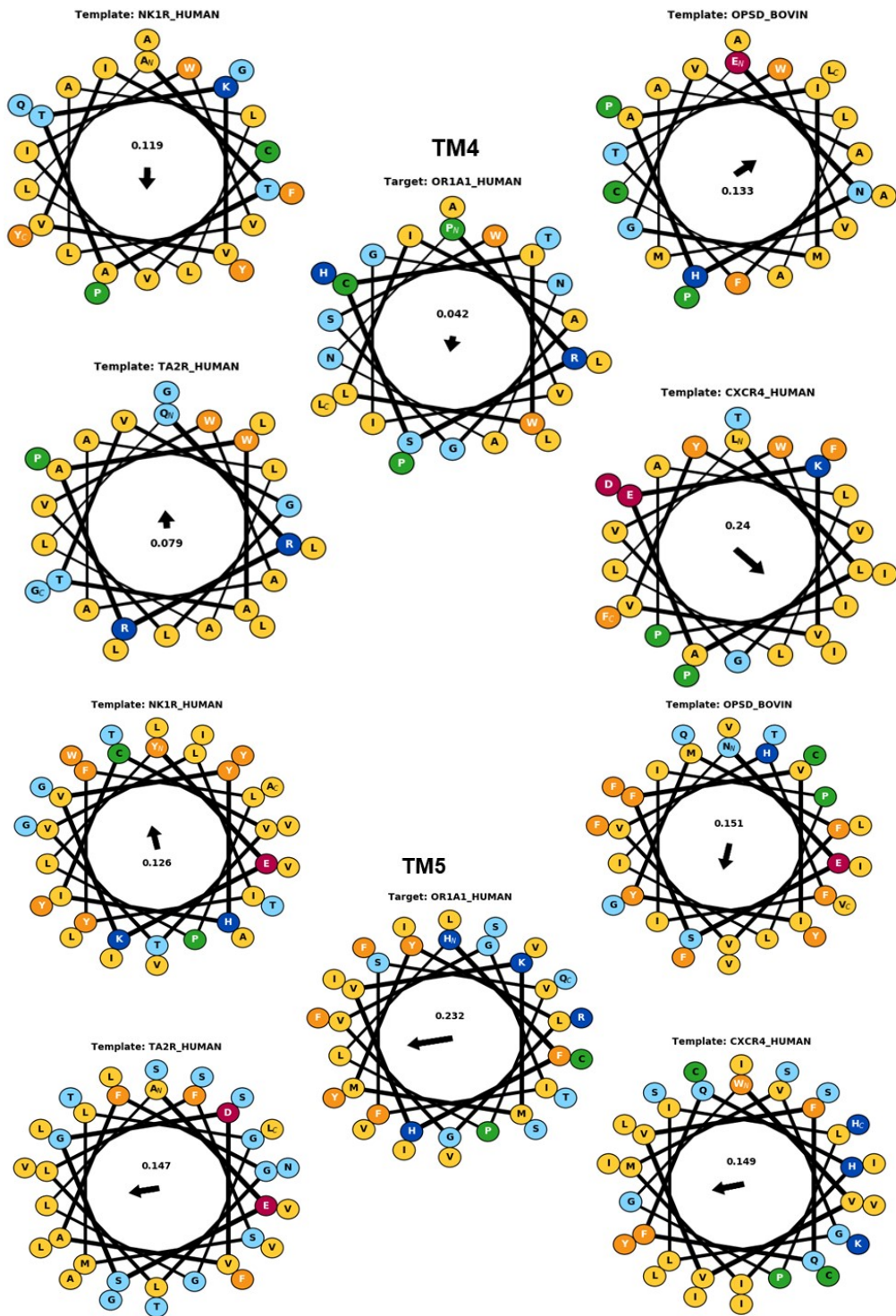
Supplementary Figure 5: Helix-wise hydrophobicity correspondence between OR1A1 and 6IIU (the 3rd best template).



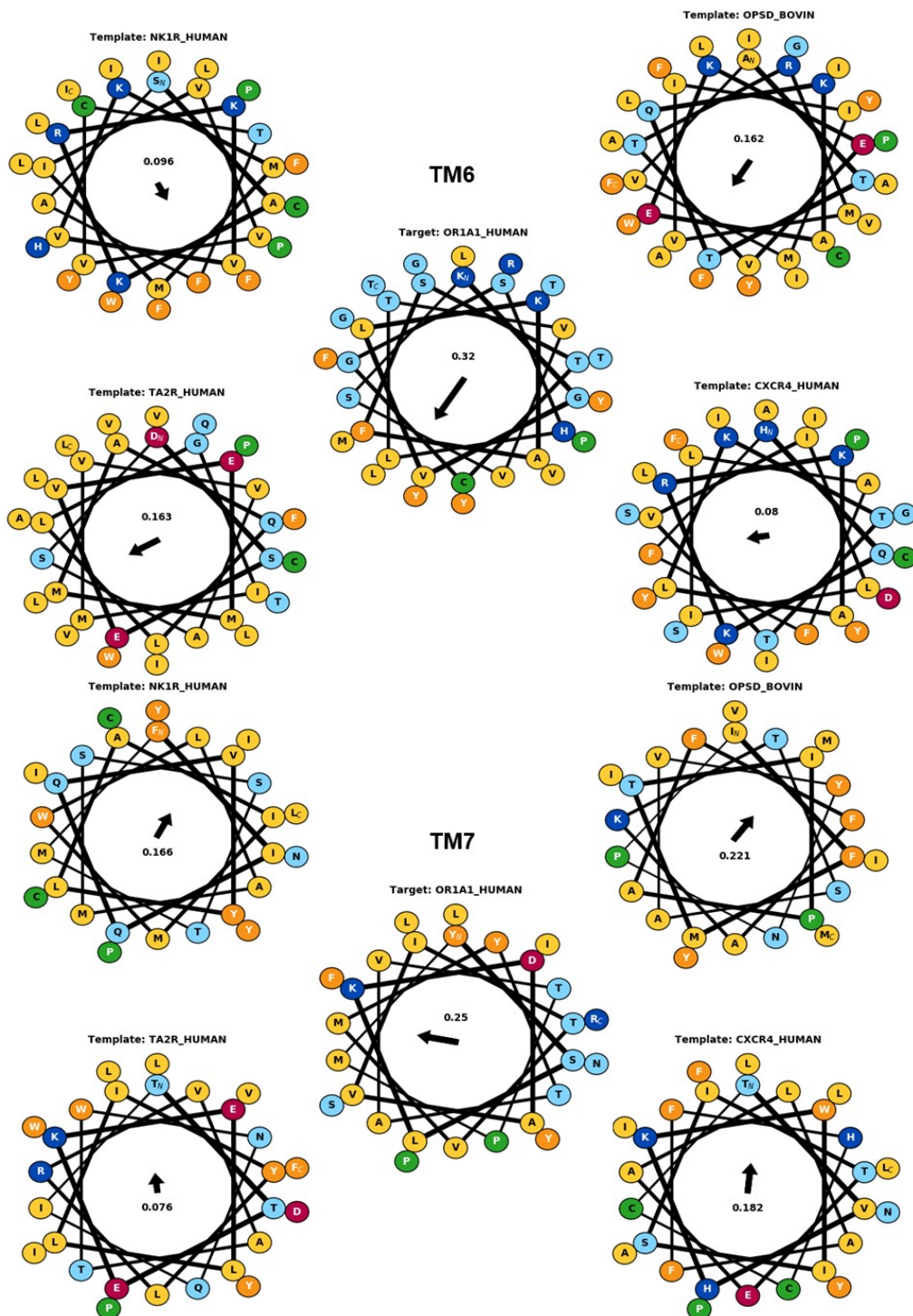
Supplementary Figure 6: Helix-wise hydrophobicity correspondence between OR1A1 and 3ODU (a template with low hydrophobicity correspondence).



Supplementary Figure 7: Helical wheel plots taken from Bio-GATS for TM2 and TM3 of target sequence (OR1A1) and the templates (NK1R_Human (6HLP), OPSD_BOVIN (1U19), TA2R_Human (6IIU), and CXCR4_Human (3ODU)). For TM3, the hydrophobic moment for OR1A1, 1U19, 6HLP, and 3ODU are pointing in almost same directions while for 6IIU, it is pointing in different directions. The hydrophobic moment for TM3 is pointing in different directions for all templates and the target.



Supplementary Figure 8: Helical wheel plots taken from Bio-GATS for TM4 and TM5 of target sequence (OR1A1) and the templates (NK1R_Human (6HLP), OPSD_BOVIN(1U19), TA2R_Human (6IIU), and CXCR4_Human (3ODU)). Within TM4, the hydrophobic moment for OR1A1 and 6HLP are pointing in same directions while for the other three it is pointing in different directions. The hydrophobic moment within TM5 for OR1A1 and all templates except 6HLP are pointing in same directions.



Supplementary Figure 9: Helical wheel plots taken from Bio-GATS for TM6 and TM7 of target sequence (OR1A1) and the templates (NK1R_Human (6HLP), OPSD_BOVIN(1U19), TA2R_Human (6IIU), and CXCR4_Human (3ODU)). The hydrophobic moment within TM6 for OR1A1 and all templates except 6HLP are pointing in same directions. For TM7 no template is showing the moment pointing in the same direction as target.

Supplementary Note S1: Bio-GATS result summary file for OPSD_BOVIN-OR1A1_HUMAN

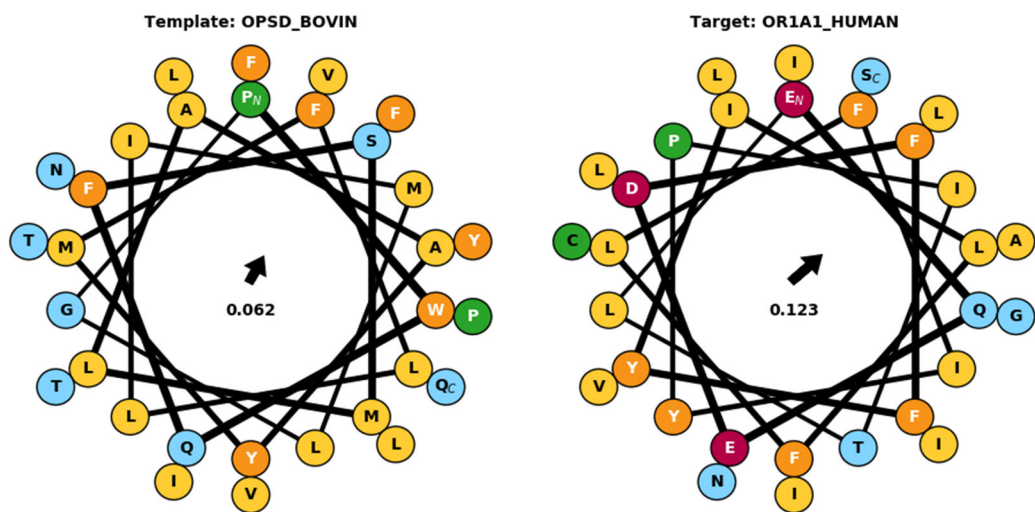
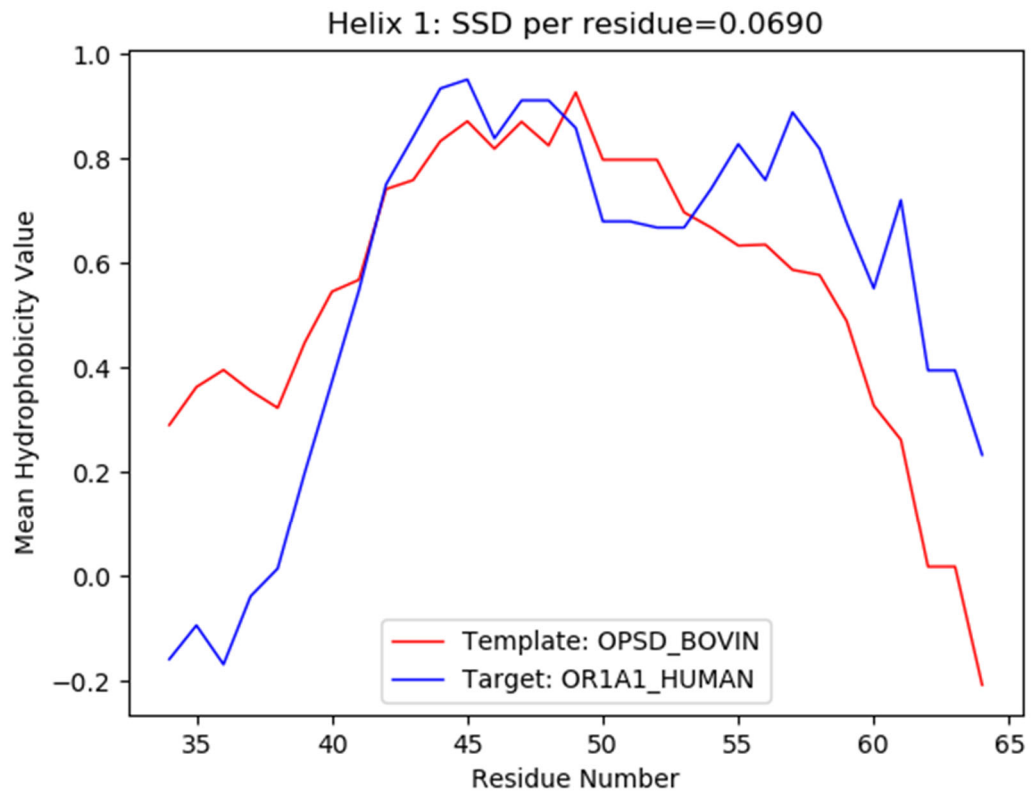
Output from OPSD_BOVIN-OR1A1_HUMAN

Please cite: Jabeen A., Ranganathan, S. BIO-GATS: A tool for automated GPCR template selection through a biophysical approach. Front. Mol. Biosci. 8:617176.

```
>OPSD_BOVIN
M--NG---T-EGPNFY---VPFSNKTGVVRSPFEAPQYYLAEPFWQFSMLAAYMFLLIMLGFPINFLTLVYVTVKKKLR
T---PPLNYILLNLAVADLFMVFGGFTTLYTSLHYF---V-FGGPTGCNLEGFFATLGGEIALWSLVLAIERYVVVC
P-----MSNFRFGE-ENHAIMGVAFTWVMALACAAPPL--GW-SRYIPEGMQCS-CG---I-DYY---TP-----
HEETNN-NESFVYMFVVHFIIPLIVIFFCYGQLVFTV--EAAQQQE-SA--ATTQKAEKEVTRMVIIMVIAFLICWLP
YAGVAFYIF-HQGSDFGP---IFMTIPAFFAKTSAVYNPVIYIMMKQFRNCMVTT---LCCG-K--NPLGDDEASTT-V
SKTETSQVAPA
>OR1A1_HUMAN
MREN-NQSSTLE---F-ILLGV----TG-----Q--Q---E--EQEDFFYILFLFIYPITLIGNLLIVLAICS--VR
-LHNPPMYFLLANLSLVDIFFSSVTIPKMLANHL---GSKSISF--FGGCLTQMYFMIALGNTDSYILAAMAYDRAVAIS
PLHYTTIMS-----PPRSCIWLIAGSWVIGNANALPHTLL--AS-----L--SFCGNQE VANFYCDITPLLKLSCSDI
H----HFHVKMMYLGVGIFSVPLLCIIVSYIRVFSTVFQ-----PS-TK---KGVLKAFSTCGSHLTVVSLYYGT
VMGTYFRPLT----Y---YSLKDAVITVMYTAVTPMLNPFIYSLR---RD-M---KAAL---RKLFN----K---RI
S----S----
```

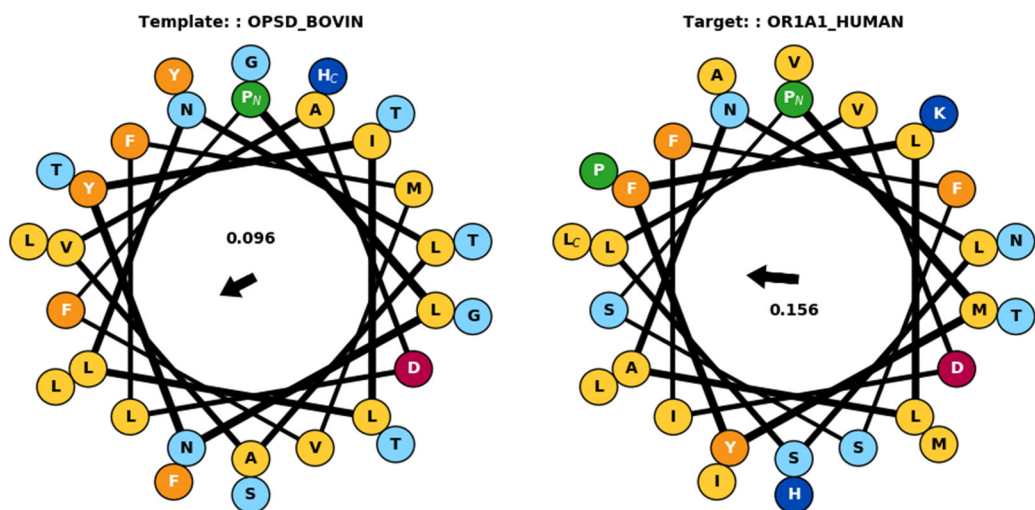
TM1

Template: PWQFSMLAAYMFLIMLGFPINFLTLVTVQ
Target: -EQEDFFYILFLFIYPITLIGNLLIVLAICS



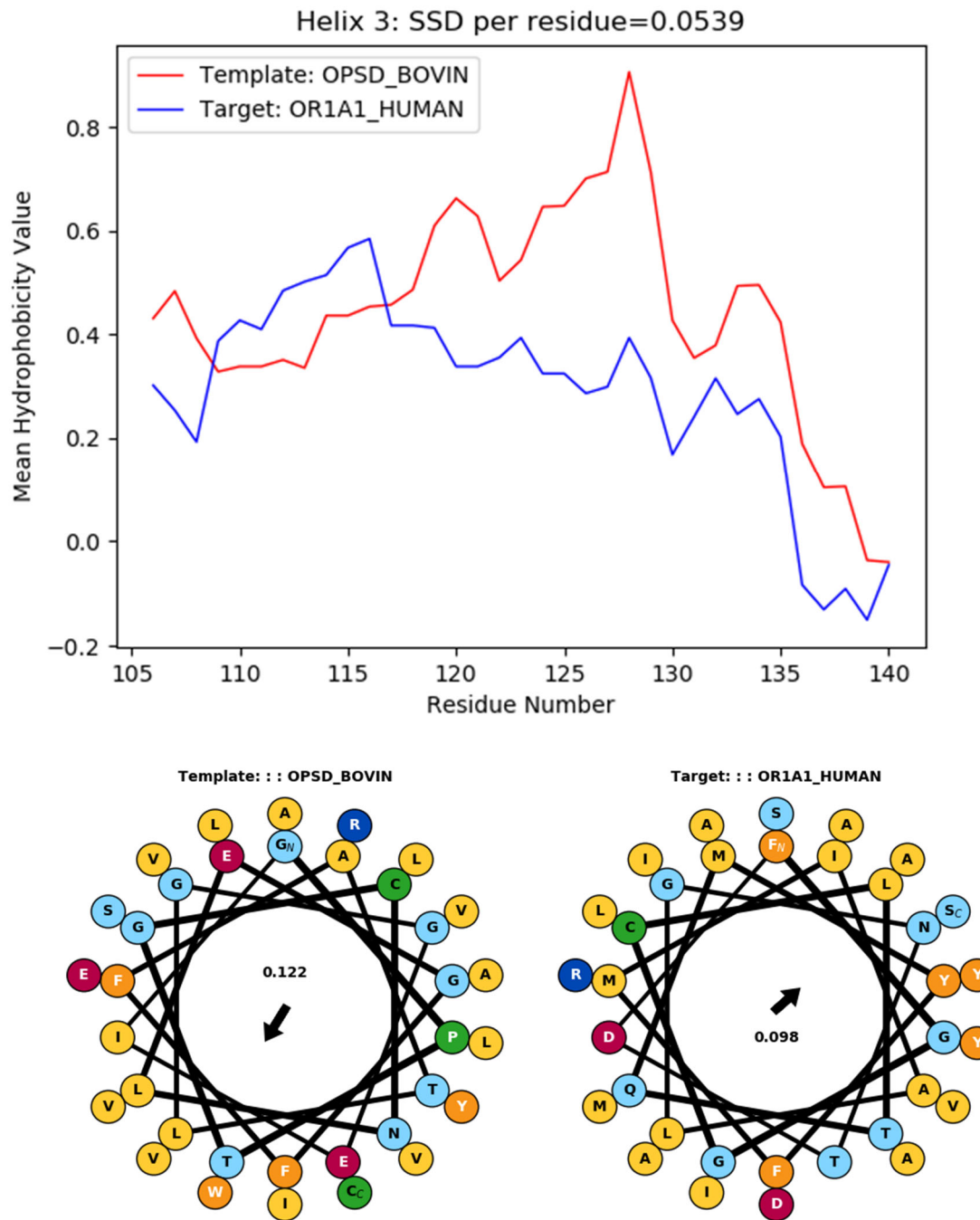
TM2

Template: PLNYILLNLAVADLFMVGFFTTLYTSLH
Target: PMYFLLANLSLVDIFFSSVTIPKMLANHL-



TM3

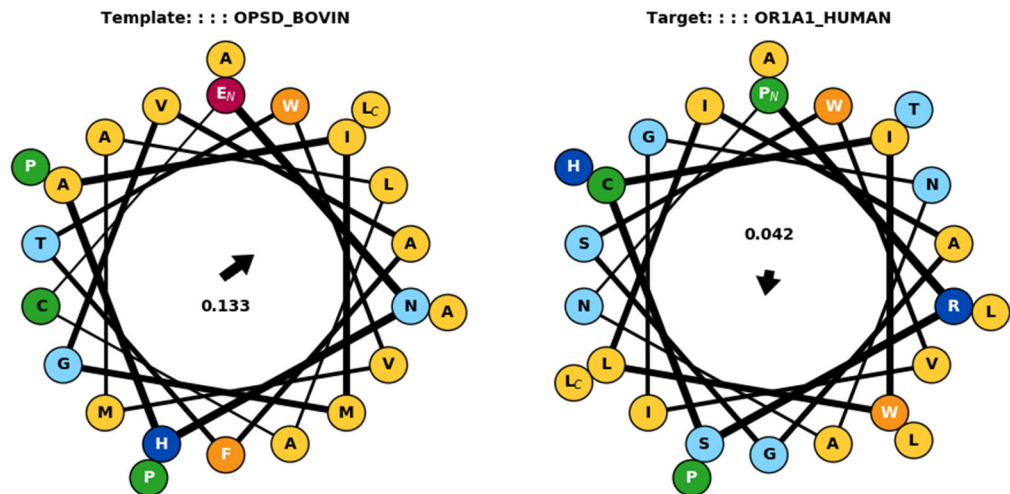
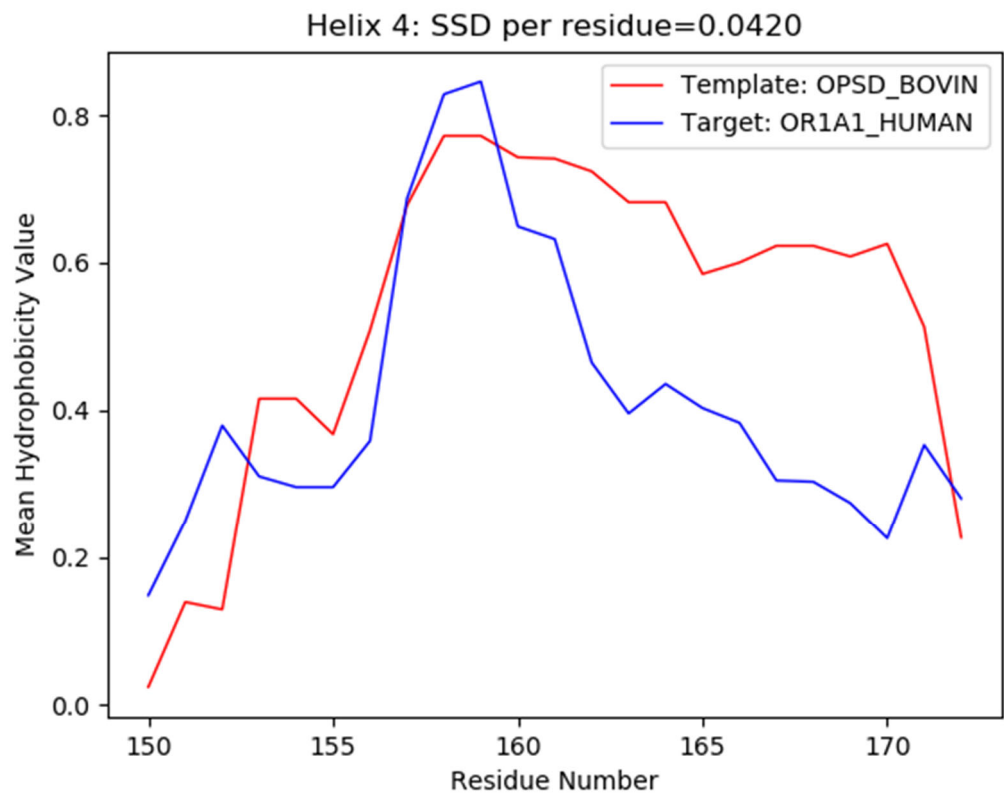
Template: GPTGCNLEGFFATLGGEIALWSLVLAIERYVVVC
 Target: -FGGCLTQMYFMIALGNTDSYILAAMAYDRAVAIS



TM4

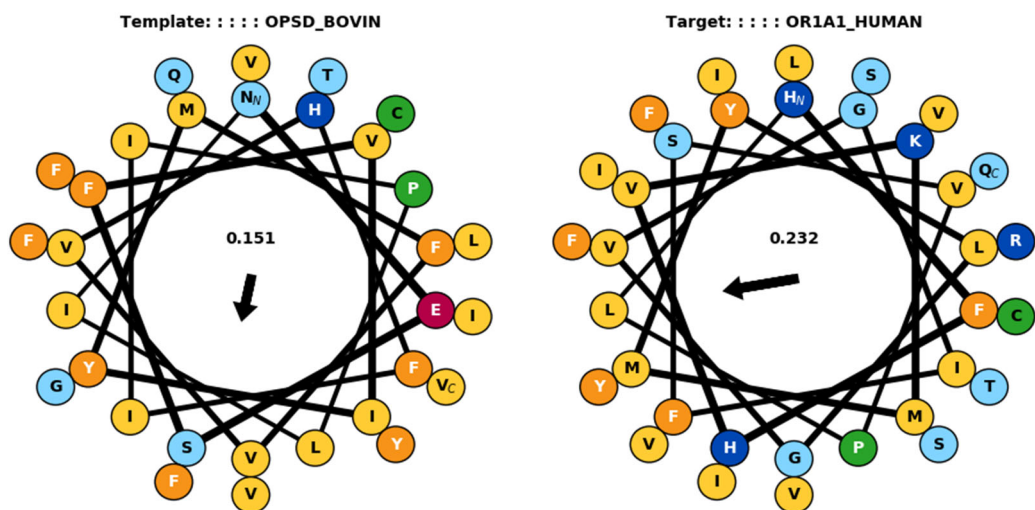
Template: ENHAIMGVAFTWVMALACAAPPL--

Target: PRSCIWLIAGSWVIGNANALPHTLL



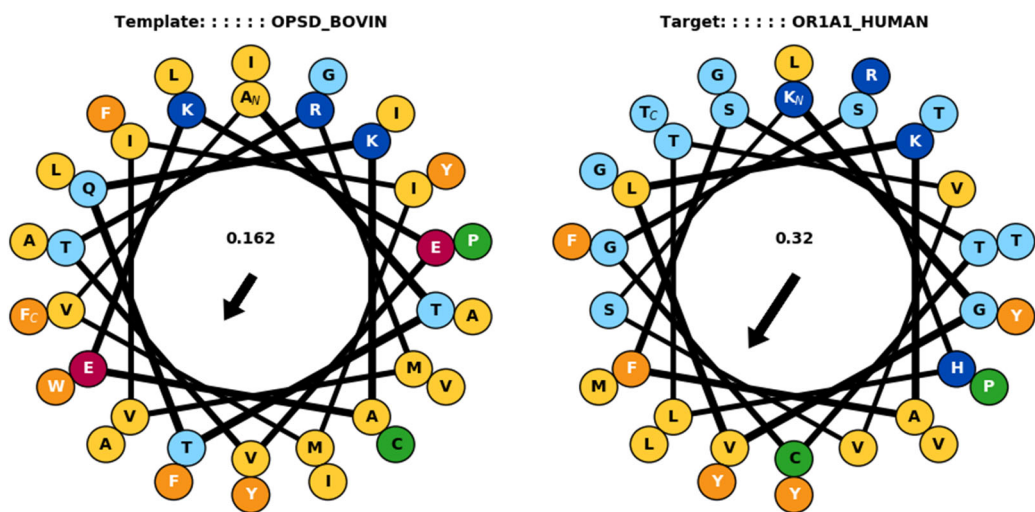
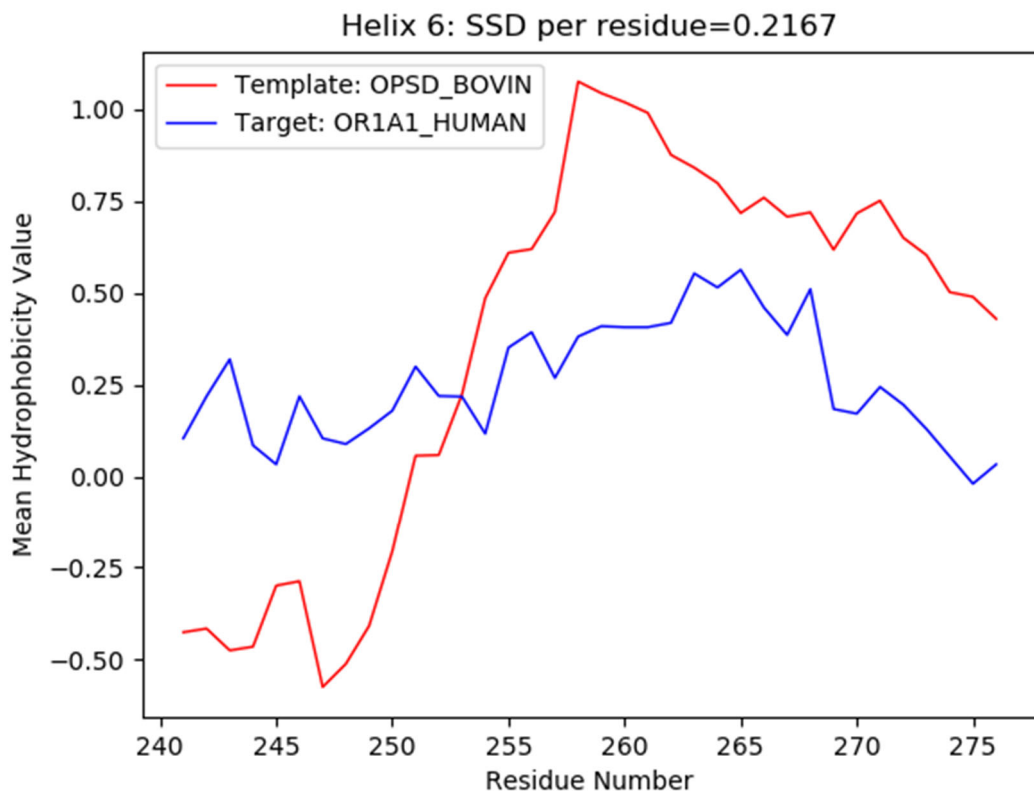
TM5

Template: -NESFVIYMFVVHFIPLIVIFFCYGQLVFTV--
Target: HFHVKKMMYLGVGIFSVPLLCIIVSYIRVFSTVFQ



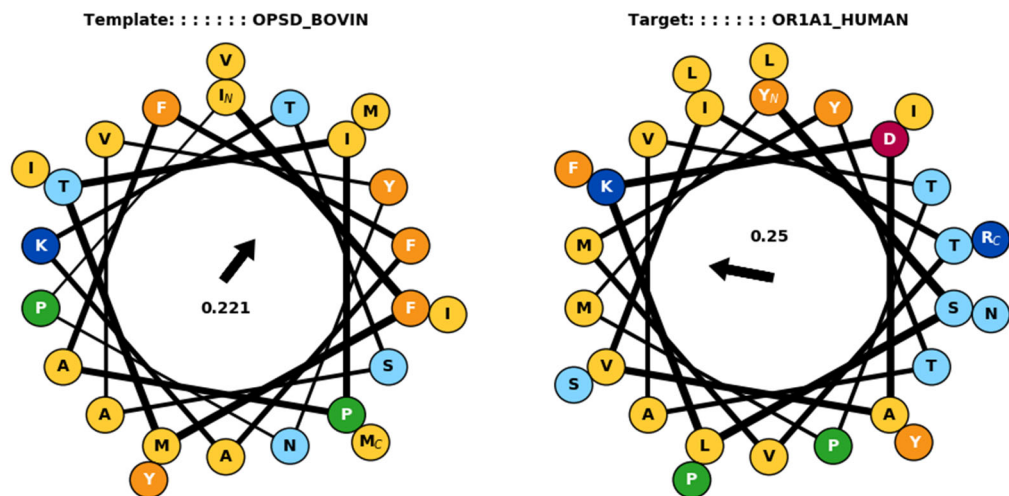
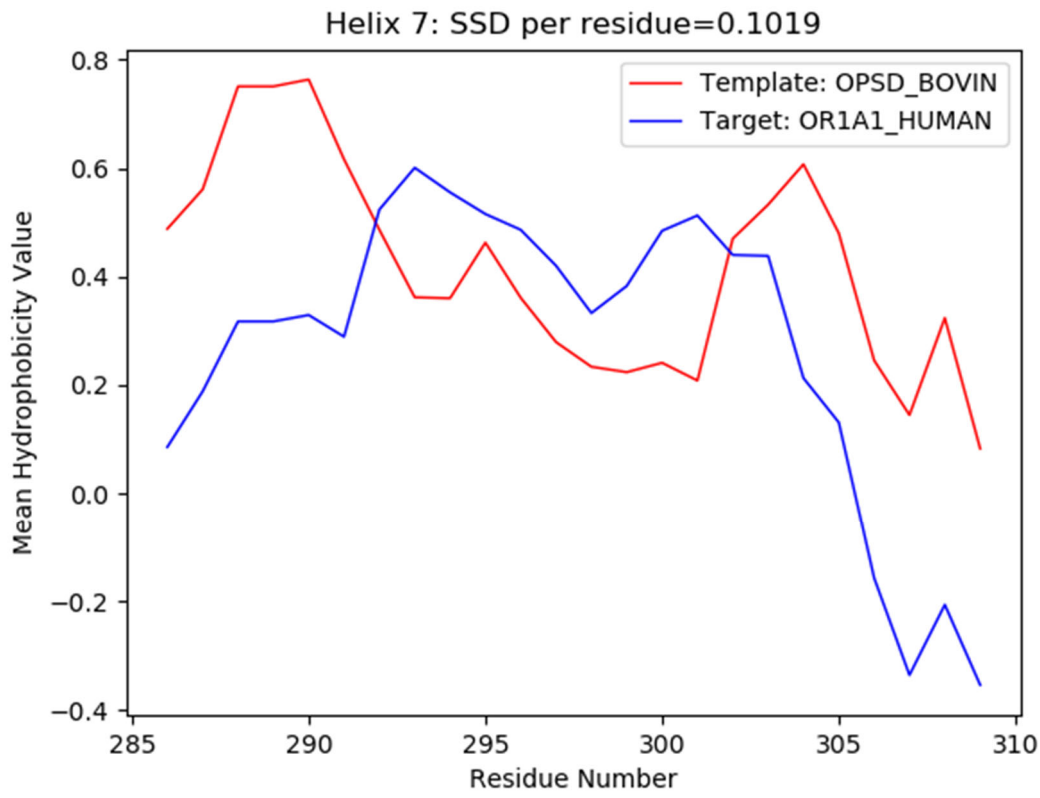
TM6

Template: ATTQKAEKEVTRMVIIMVIAFLICWLPYAGVAFYIF
Target: ----KGVLKAFSTCGSHLTVVSLYYGTVMGTYFRPLT



TM7

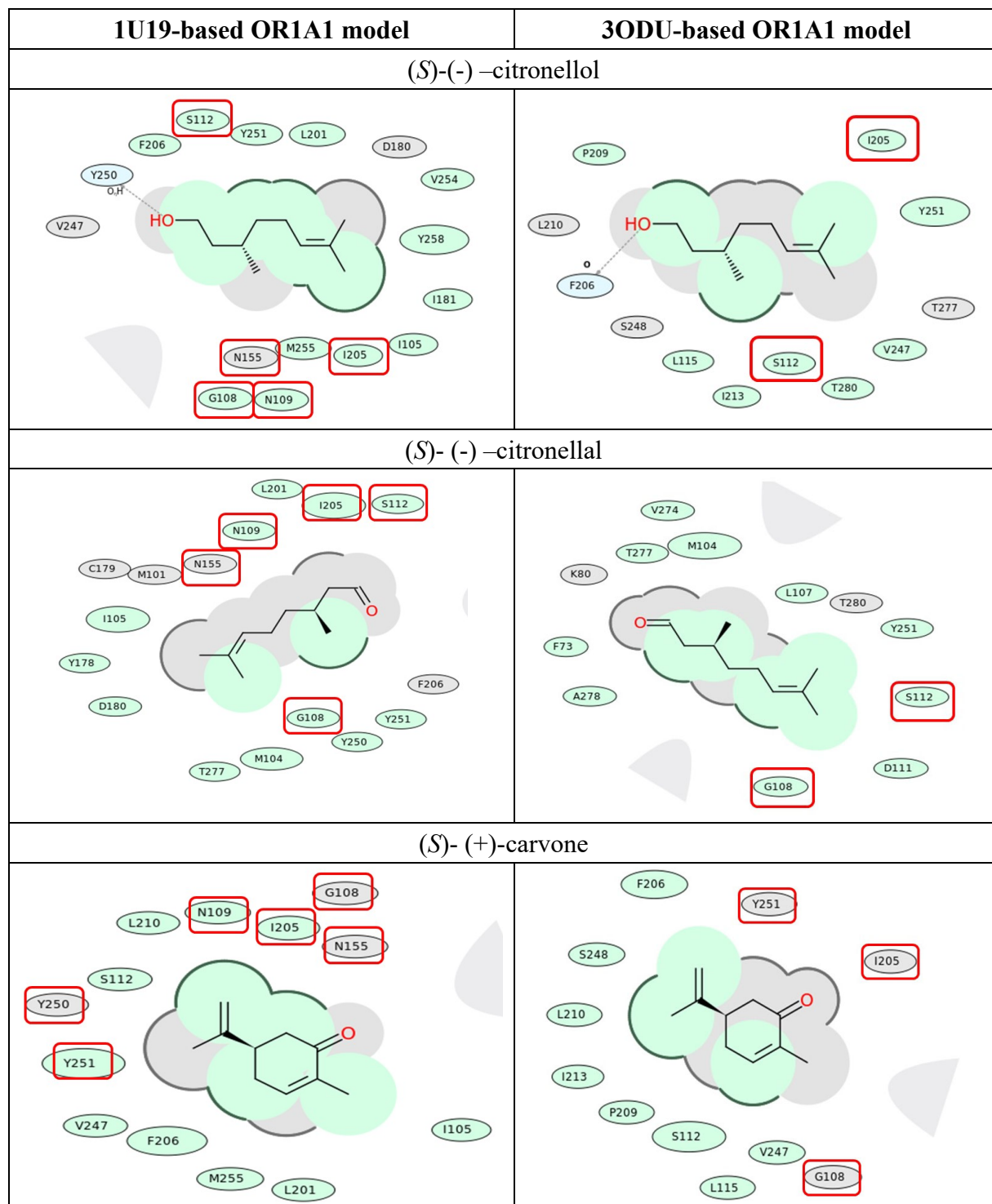
Template: ---IFMTIPAFFAKTSAYVNPIYIMM
Target: YSLKDAVITVMYTAVTPMLNPFYSLR



Supplementary Table 4: Ligand profile comparison between OR1A1 and the selected templates

No.	OR1A1 ligands	PubChem ID	No.	OR1A1 ligands	PubChem ID
1	(S)-(-)-citronellal	443157	31	Quinoline	7047
2	4-decenal	61875	32	R-limonene	440917
3	(S)-(-)-citronellol	7793	33	(R/S)-octen-3-ol	6992244
4	(R)-(+)-citronellol	75427	34	2-pentylpyridine	16800
5	(S)-(-)-limonene	439250	35	2-phenylethanethiol	78126
6	Z-7-decanal	5362695	36	2-Phenylethyl acetate	7654
7	Nerolidol	5284507	37	3-Mercaptohexyl acetate	518810
8	E-4-decanal	5702654	38	Estragole	8815
9	Nerol	643820	39	Ethyl cyclohexane-carboxylate	18686
10	Helional	64805	40	Trans-Anethole	637563
11	(-)-Carveol	11084068	41	3-Methyl-2,4-nonanedione	529481
12	Allyl heptanoate	8878	42	Ethylphenyl acetate	7590
13	Ethyl hexanoate	31265	43	5-Pentyloxolan-2-one	7710
14	(-)-Carvone	439570	44	(+)-Menthone	443159
15	(+)-Dihydrocarvone	22227	45	Musk xylol	62329
16	1-decanol	8174	46	Cosmone	66823518
17	2-octanone	8093	47	Celestolide	61585
18	3-heptanone	7802	48	2-ethylphenol	6997
18	3-octanone	246728	49	Methyl isoeugenol	7128
20	4-chromanone	68110	50	P-Tolyl isobutyrate	7685
21	Allyl phenylacetate	15717	51	Propiophenone	7148
22	Benzophenone	3102			
23	Benzyl acetate	8785			
24	Dihydrojasmone	62378			
25	Nonanethiol	15077			
26	(+)-Carvone	16724			
27	3-phenyl propyl propionate	61052			
28	Androstadienone	92979			
29	Butyl anthranilate	24433			
30	Cinnamaldehyde	637511			

Supplementary Table 5: The interactions of 1U19-based and 3ODU-based OR1A1 models with known ligands of OR1A1 with mutagenesis data. Hydrophobic regions in green, van der Waals interactions in grey surface accessible regions in grey parabolas; hydrogen bond acceptors in blue. The residues having mutagenesis data are boxed in red.



The figure displays four panels comparing protein-ligand docking results for three molecules using two different OR1A1 models: 1U19-based (left) and 3ODU-based (right).

- (R)-(-)-carvone:** The ligand is a bicyclic monoterpene. In the 1U19 model, residues L210, N109, I205, N155, Y250, Y251, V247, F206, M255, I105, and L201 are shown. In the 3ODU model, residues F206, S248, L210, I213, P209, S112, V247, L115, G108, and Y251 are shown.
- Musk tibetene:** The ligand is a polycyclic aromatic compound with nitro groups. In the 1U19 model, residues Y258, V254, L201, F206, M255, Y251, I205, N109, G108, S112, T277, I181, I105, D180, M104, T280, Y250, and V255 are shown. In the 3ODU model, residues I181, N176, Y258, G204, L205, F177, M255, V274, A175, T277, G108, M104, N109, L107, and Y251 are shown.
- Musk xylene:** The ligand is a polycyclic aromatic compound with nitro groups. In the 1U19 model, residues Y258, V254, M255, L201, F206, I205, Y251, G108, S112, T280, Y250, I109, I210, L181, I105, D180, M104, T277, and I205 are shown. In the 3ODU model, residues L244, I214, V247, L115, I213, P209, L210, S112, I205, F206, S248, M255, G252, and Y251 are shown.

3EML_A OR1A1	-----IMGSS-----VYITVELAIAAVLAILG N VLVCWAWLNSNLQNVTN 40 MRENNQSSTLEFILLGVTQQEQEDFFYILFLFIYPITLIG N LLIVLAICSDVRLHNP M 2.50 3EML_A OR1A1 YFVVSLAA A DIAVGVLAIP--FAITISTGFCAACHGCLFIACFVLVLTQSSIFSLLAIAI 98 FLLANLSLV D IFFSSVTIPKMLANHLLGSKSISFGGCLTQMYFMIALGNTDSYILAAMAY 120 3.50 3EML_A OR1A1 D RYIAIRIPLRYNGLVTGTRAKGIIAIC W VLSFAIGLTPMLGWNNCGQSQGC G E Q VACL 158 DRAVAISRPLHYTTIMSPRSCIWLIAGS W VIGNANALPHTLLTASLS---FCGNQE V ANF 177 5.50 3EML_A OR1A1 F EDVVPMNYMVYFNFFACVLVPLL---LMLGVYLRIFLAARRQLRSTLQKEVHA A KSLAI 215 YCDIT P LKKLSCSDIHFKMMYLGVGIFSV P LLCIIVSYIRVFSTVFQVPSTKGVLKAF 237 6.50 3EML_A OR1A1 IVGLFALCW L PLHIINCFTFFCPDCSHAPLWLMYLAIVLSHTNSV V NPF I YAYRIREFRQ 275 STCGSHLTVVSLYYGTVMGTYFRPLTNYSLKDAVITVMYTAVTPMLNPF I YSLRN R DMKA 297 3EML_A OR1A1 TFRKII R SHVLRQ 288 ALRKLFNKR I SS- 309	1.50
-----------------	---	------

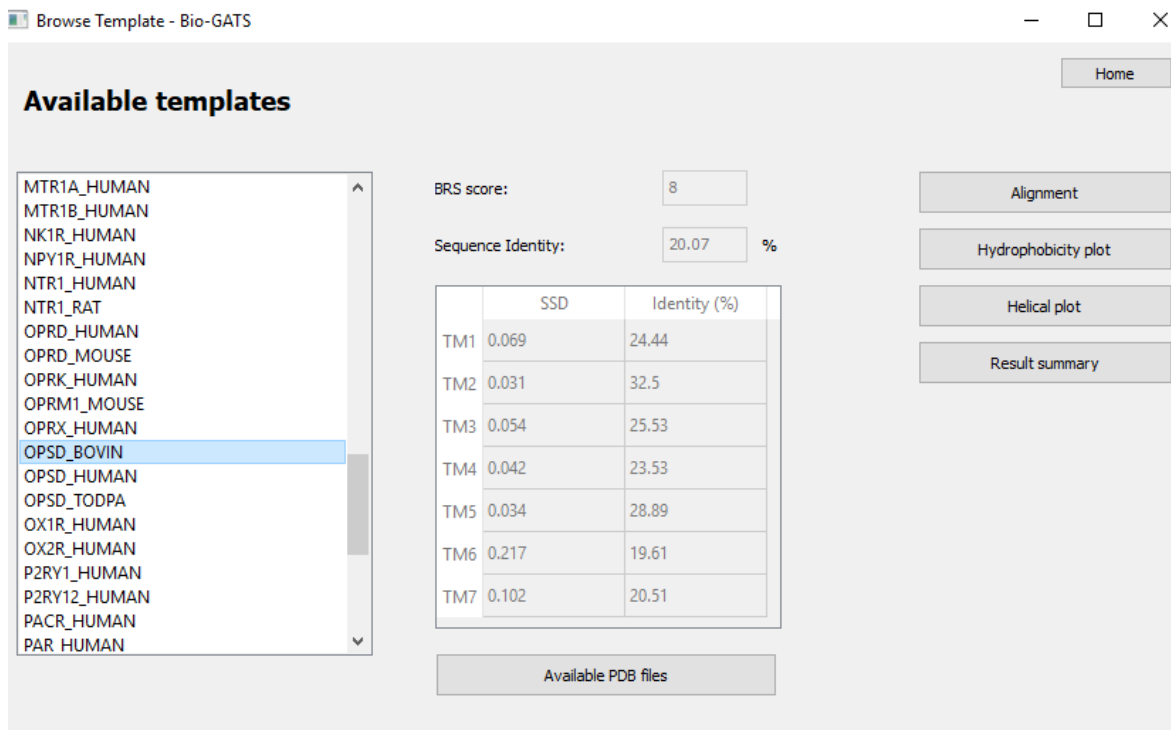
Supplementary Figure 10: The alignment generated by GPCR-I-TASSER between query sequence (OR1A1) and the top template (3EML). The center TM residues in each sequence are in red colour.

3EML OR1A1	-----IMGSSVYITVELAIAAVLAILG N VLVCWAWLNSNLQNVTN 40 MRENNQSSTLEFILLGVTQQEQEDFFYILFLFIYPITLIG N LLIVLAICSDVRLHNP M 2.50 3EML OR1A1 YFVVSLAA A DIAVGVLAIPFAITISTG--FCAACHGCLFIACFVLVLTQSSIFSLLAIAI 98 FLLANLSLV D IFFSSVTIPKMLANHLLGSKSISFGGCLTQMYFMIALGNTDSYILAAMAY 120 3.50 3EML OR1A1 D RYIAIRIPLRYNGLVTGTRAKGIIAIC W VLSFAIGLTPMLGWNNCG----QSQGC G E 153 DRAVAISRPLHYTTIMSPRSCIWLIAGS W VIGNANAL-PHTLLTASLSFCGNQE V ANFYC 179 5.50 3EML OR1A1 Q VACLFEDVVPMNYMV---YFNFFACVLV P LLLMLGVYLRIFLAARRQLRSTLQKEVHAA 210 DITPLKKLSCSDIHFKMMYLGVGIFSV P LLCIIVSYIRVFSTVFQ-----V 227 6.50 3EML OR1A1 KSLAIIVGLFALCW L PLHIINCFTFF-----CPDCSHAPLWLMYLAIVLSHTNSV V NPF 264 PSTKGVLKAFSTCGSHLTVVSLYYGTVMGTYF-RPLTNYSLKDAVITVMYTAVTPMLNPF 286 3EML OR1A1 IYAYRIREFRQTFRKII R SHVLRQ 288 IYSLRN R DMKAALRKLFNKR I SS- 309	1.50
---------------	---	------

Supplementary Figure 11: The alignment generated by GPCRM between query sequence (OR1A1) and the top template (3EML). The center TM residues in each sequence are in red colour.

OPSD_BOVIN	M--NG----T-EGPNFY----V PFSNK TGVVRSPFEAPQYYLAEPWQFSMLAAYMFLLI	39
OR1A1_HUMAN	MREN-NQSSTLE---F-ILLGV----TG-----Q--Q---E--EQEDFFYILFLFIY	35
	1.50	2.50
OPSD_BOVIN	MLGFPINFLTLVYTVQKKLRT---PPLNYILLNLAVADLFMVFGGFTTLYTSLHYF---	93
OR1A1_HUMAN	PITLIGNLLIVLAICS--VR-LHNPPMYFLLANLSLVDIFFSSVTIPKMLANHL---GSK	90
	3.50	
OPSD_BOVIN	-V-FGGPTGCNLEGFFATLGGEIALWSLVVLAIE R YVVVCP-----MSNFRFGE-ENHA	144
OR1A1_HUMAN	SISF--FGGCLTQMYFMIALGNTDSYILAAMAYD R AVAISPLHYTTIMS-----PPRSC	141
	4.50	
OPSD_BOVIN	IMGVAFT W VMALACAAPPL--GW-SRYIPEGMQCS-CG---I-DYY---TP-----	184
OR1A1_HUMAN	IWLIAGS W VIGNANALPHTLL--AS-----L--SFCGNQE V ANFYCDITPLLKLSCSDI	192
	5.50	
OPSD_BOVIN	HEETNN-NESFVIYMFVVFHII P LIVIFFCYGQLVFTV--EAAAQQQE-SA--ATTQKAE	238
OR1A1_HUMAN	H----HFHVKKMMYLGVGIFSV P LLCIIVSYIRVFSTVFQ-----PS-TK---KGV	233
	6.50	7.50
OPSD_BOVIN	KEVTRMVIIMVIAFLICWL P YAGVAFYIF-HQGSDFGPI---IFMTI P AFFAKTS A VYN P	294
OR1A1_HUMAN	LKAFSTCGSHLTVVSLYYG T VMGTYFRPLT-----Y---YSLKD A ITV M YTAVTPMLN P	285
	VIYIMMKQFRNCMVTT---LCCG-K--NPLGDDEASTT-VSKTETSQVAPA	338
OPSD_BOVIN	FIYSLR---RD-M---KAAL---RKLFN-----K---RIS---S-----	309
OR1A1_HUMAN		

Supplementary Figure 12: The alignment generated by BIO-GATS between the query sequence (OR1A1) and the selected template, 1U19. The center TM residues in each sequence are in red colour.

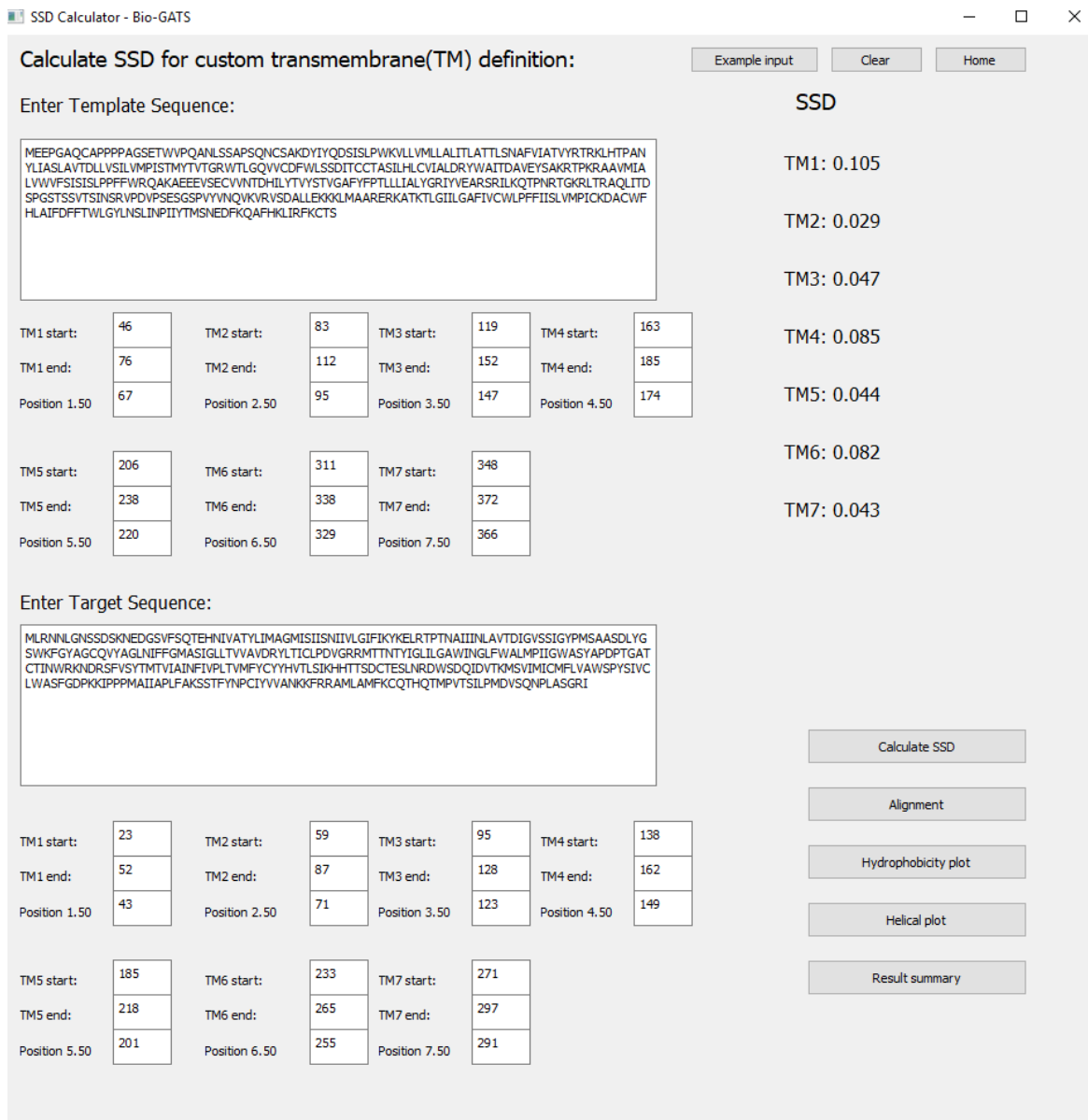


Supplementary Figure 13: The *Browse template* window with options for showing alignment, downloading hydrophobicity plots, helical wheel plots, and viewing available PDB data for each receptor. HC in terms of SSD, global sequence identity, TM-wise sequence identity, and binding site residue similarity (BRS) score are computed upon receptor selection.

The screenshot shows a window titled "Available PDBs" with a list of 12 entries. The entries are displayed in a table with columns: PDBID, Resolution, and Position. The first entry, "6H7N", is highlighted with a dashed border. The "Position" column contains ranges such as "44-368" and "33-368". A vertical scroll bar is visible on the right side of the table.

	PDBID	Resolution	Position
1	6H7N	2.5	44-368
2	6H7O	2.8	44-368
3	6H7L	2.7	44-368
4	6H7J	2.8	44-368
5	6H7M	2.8	44-368
6	5F8U	3.4	33-368
7	5A8E	2.4	33-368
8	4BVN	2.1	33-368
9	3ZPR	2.7	33-368
10	3ZPQ	2.8	33-368
11	4GPO	3.5	33-368
12	4AMI	3.2	33-368

Supplementary Figure 14: The *Available PDBs* window, showing the PDB data for OPSD_MELGA



Supplementary Figure 15: The *SSD calculator* with customizable TM definitions.

Alignment - Bio-GATS

Close

OPSD_BOVIN-OR1A1_HUMAN

TM1	OPSD_BOVIN OR1A1_HUMAN	34 22	PWQFSMLAAYMFLIMLGFPINFLTLYYVTQ -EQEDFFYILFLFIYPITLIGNLLIVLAICS	64 51
TM2	OPSD_BOVIN OR1A1_HUMAN	71 58	PLNYILLNLAVADLFMVFGGFTTLYTSLH PMYFLLANLSLVDIFFSSVTIPKMLANHL-	100 86
TM3	OPSD_BOVIN OR1A1_HUMAN	106 94	GPTGCNLEGFFATLGGEIALWSLVLAIERYVVVC -FGGCLTQMYFMIALGNTDSYILAAMAYDRAVAIS	140 127
TM4	OPSD_BOVIN OR1A1_HUMAN	150 138	ENHAIMGVAFTWVMALACAAPPL-- PRSCIWLIAAGSWVIGNANALPHTLL	172 162
TM5	OPSD_BOVIN OR1A1_HUMAN	200 193	-NESFVIYMFVVHFI IPLIVIFFCYGQLVFTV-- HFHVKKMMYLGVGIFSVPLLCIIVSYIRVFSTVFQ	230 226
TM6	OPSD_BOVIN OR1A1_HUMAN	241 231	ATTQKAEKEVTRMVIIMVIAFLICWL PYAGVAFYIF-- ---KGVLKAFSTCGSHLTvvSlyyGTVMTYFRPLT	276 263
TM7	OPSD_BOVIN OR1A1_HUMAN	286 265	---IFMTI PAFFAKTS A VYNPVIYIMM YSLKDAVITV MYTA VT PMLNPFIYSLR	309 291

[Download TM-wise Alignment](#) [Download Full Alignment](#)

Supplementary Figure 16: The *Show alignment* window displaying the helix-wise alignment between OPSD_BOVINE and OR1A1

Supplementary References

1. Perry, S.R., W. Xu, A. Wirija, J. Lim, M.K. Yau, M.J. Stoermer, A.J. Lucke, and D.P. Fairlie, *Three Homology Models of PAR2 Derived from Different Templates: Application to Antagonist Discovery*. *J Chem Inf Model*, 2015. **55**(6): p. 1181-91.
2. Shahaf, N., M. Pappalardo, L. Basile, S. Guccione, and A. Rayan, *How to Choose the Suitable Template for Homology Modelling of GPCRs: 5-HT7 Receptor as a Test Case*. *Mol Inform*, 2016. **35**(8-9): p. 414-23.
3. Loo, J.S., A.L. Emtage, K.W. Ng, A.S. Yong, and S.W. Doughty, *Assessing GPCR homology models constructed from templates of various transmembrane sequence identities: Binding mode prediction and docking enrichment*. *J Mol Graph Model*, 2018. **80**: p. 38-47.
4. Castleman, P.N., C.K. Sears, J.A. Cole, D.L. Baker, and A.L. Parrill, *GPCR homology model template selection benchmarking: Global versus local similarity measures*. *J Mol Graph Model*, 2019. **86**: p. 235-246.
5. Jaiteh, M., I. Rodríguez-Espigares, J. Selent, and J. Carlsson, *Performance of virtual screening against GPCR homology models: Impact of template selection and treatment of binding site plasticity*. *PLoS Comput Biol*, 2020. **16**(3): p. e1007680.